Gregory Pitner
Mentors: Michelle Rincon & Robert Chen
Instructor: Prof. Roger Howe
Academic Advisor: H.-S. Philip Wong
EE 412 Final Report – Fall 2015
10 December 2015

Aligned Carbon Nanotube Growth using FirstNano CVD Furnace in Stanford Nanofabrication Facility

Abstract

This project continues work that started in February 2015, when a FirstNano "EasyTube 3000" Carbon Nanotube (CNT) growth furnace was installed in the Stanford Nanofabrication Facility (SNF). The tool features a high level of automation and process control built into an easy-to-use software environment. The purpose of the tool is to grow horizontally aligned or unaligned single-walled carbon nanotubes, and is capable of vertical forest CNT growth if future users desire it. This report summarizes the efforts to create a turn-key solution for aligned carbon nanotube growth in the Stanford Nanofabrication Facility (SNF). The previous quarter focused on creating recipes with Methane carbon precursor, and this work focuses on using Ethanol as the precursor for CNT growth. We have 1) defined a wafer-scale sample preparation process using tools sourced within the SNF and explored the CVD growth parameters that give the best growth, 2) demonstrated the consistency and turn-key capability of the furnace by growing CNTs with reproducibly 5-10 CNT/um density every single time across much more than dozens of separate samples, and 3) demonstrated the 100mm wafer-scale uniformity of the CNT growth as well as performed materials and electrical characterization to confirm the useful properties of the as-grown CNTs.

Motivation

Single-walled Carbon Nanotubes (CNTs) are strong candidates for applications in high-performance and energy-efficient electronics, monolithically heterogeneously integrated computing architectures, and sensor networks or biological interfaces. Specifically, in VLSI electronics a 10x improvement in energy-delay-product, a metric of energy efficiency and performance, is projected to occur for systems on the sub-7nm technology node based on transistors with semiconducting CNT channels. Uniquely, the low-temperature CNT transfer decouples high temperature CVD growth from temperature-sensitive device processing thereby enabling transistor logic to be placed at multiple levels of a monolithically integrated circuit and to co-exist with other low-temperature device or memory technologies in future heterogeneous architectures. CNTs also make great sensors, and are being considered as possible electrical interfaces to biological materials such as cells or neurons. The leading materials platform for these applications are horizontally aligned single-walled carbon nanotubes that are grown in a chemical vapor deposition (CVD) process. The preferred growth technique is the perfectly aligned parallel arrays of CNTs on quartz substrates, before transfer to the device fabrication substrate. Due to this project, the SNF now has this capability.

CNT Growth Mechanisms, Sample Preparation and Growth Process Overview

The aligned CVD growth process for Single-walled carbon nanotubes has been used in various forms for more than a decade, and the mechanisms involved have been studied extensively across a range of substrates, catalyst materials, carbon sources, and growth conditions in hundreds of publications. Here, we summarize the key mechanisms involved in horizontally aligned CNT growth.

A cartoon of these mechanisms alongside a growth example is shown in Figure 1. First, a thin film (2-4Å) of metal (possibly Fe, Ni, Cu, Co, etc… we use Fe) is deposited by evaporation in a lithographically patterned catalyst region. During evaporation the film grows as sub-monolayer islands of metal according to Volmer-weber mechanism. These islands are annealed at high temperatures in the presence of hydrogen and coalesce into the nanoparticles with diameters of a few nanometers. Next, at high temperature a carbon containing gas (CH_4, C_2H_6O, C_3H_8O, etc...) decomposes catalytically at the catalyst nanoparticle into the reactant carbon gas species. This reactive carbon species coats the nanoparticle morphology to form a hemispherical CNT end-cap through either a direct surface assembly (Vapor-Solid mechanism) or subsurface diffusion into the nanoparticle bulk before precipitating out and forming a surface assembly (Vapor-Liquid-Solid mechanism). This end-cap is then extended by the addition of subsequent carbon blocks into a longer tube of carbon thereby building the CNT. The structure of the carbon nanotube is partially determined by the catalyst particle size, and is randomly distributed between the possible CNT chiralities to give approximately 2/3rds fraction semiconducting CNTs and the rest metallic. Growth mechanisms to enhance the purity of the semiconducting CNT fraction by direct chiral selective growth or selective metallic CNT removal exist and may be introduced in future evolutions of this tool's process. Finally, when grown on certain substrates (Quartz, Sapphire, a few others) the CNTs interact with the crystal lattice which imparts an angle-dependent Van der Waals force on the CNT along certain crystal lattice directions. For ST-cut Quartz, this aligns the CNT along the [100] plane.

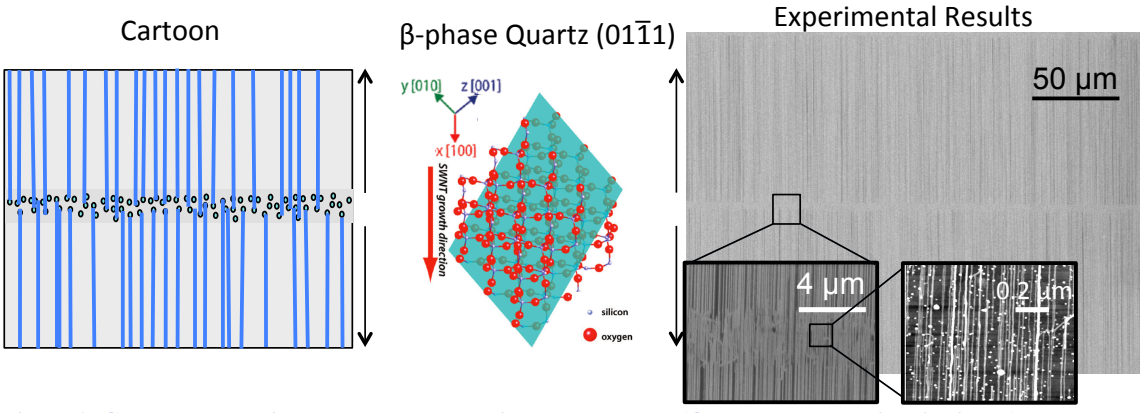

Figure 1: Growth Mechanism cartoon and experimental example. (Quartz crystal lattice citation: A. Rutkowska, et. al. 2009)

Sample Preparation

The sample preparation process is summarized in Figure 2, and the fabrication details are contained in this paragraph. Further details are included in the appendix and a process run-sheet will be distributed to labusers during tool training. The 100mm quartz substrates wafers used are single-side polished ST-cut Quartz with an angle of 42°45'

sourced from Hoffman Materials, LLC. These substrates are now stocked in the SNF stockroom. First the quartz is solvent-cleaned then annealed in Tylan9 at 900°C for 8 ½ hours using the recipe "SLO900O". Next, use Headway to spin on LOL2000 (a liftoff under-cut layer) at 3000 RPM for 60 seconds to obtain an ~200nm layer. Bake the LOL in the oven near LithoSolvent bench at 200°C for 30 minutes. Use SVG coat track 2 to coat 1um of Shiply 3612 without vapor prime and without any edge-bead-removal. Do not use spin-rinse-dry on the quartz wafers like you would normally do after resist coating, as the wafers are fragile compared to silicon and may crack. Using ASML, expose the catalyst pattern (user-defined, but the legacy baseline is 4um wide stripes with a pitch of 100um) with a dose of ~150 mJ/cm^2, and develop in SVG Develop using program 5 without pre- or post- develop bakes. The catalyst deposition is the only part of the process not performed inside the SNF. Stanford researchers can use Tom Carver as a vendor in the SNSF, for a fee he will deposit 3.2Å Fe catalyst at 0.33Å/s for optimal results. Non-Stanford labusers can use the Innotec evaporator, or in the future the AJA evaporator that will be brought online in 2016 to deposit their catalyst. User optimization of the catalyst is required, and the optimal thickness and rate value may change based on future process improvements. (Note: We recommend users do not use Innotec for catalyst evaporation due to the lack of a crystal monitor reading before the shutter opens and deposition begins, which is why we do not currently do catalyst depositions in SNF.) After catalyst evaporation, liftoff catalyst in two acetone baths for longer than 10 minutes each at WB-solvent, followed by an MF-26A bath and multiple DI water baths at WB-Miscres. After the last DI water bath, rinse wafer with IPA and blow-dry with an N2 gun. Inspect samples for any photoresist residue, and if it is clean the sample is now ready for growth in the FirstNano CNT CVD Growth Furnace!

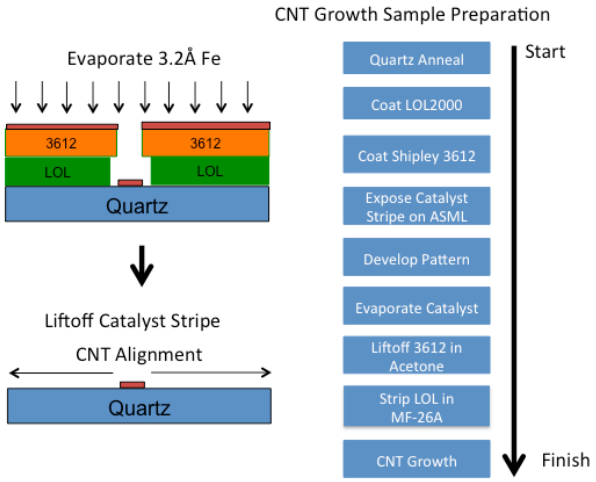

Figure Figure 2: Sample Preparation Process Flow

Alternative sample preparation strategies exist with similar results, including a blanket evaporation and etch process that can be cleaner than liftoff approach, however it has never matched the density of the liftoff approach.

CNT CVD Growth Procedure

The CVD growth procedure has four distinct phases as shown in figure 3: 1) Calcination, 2) Reduction, 3) CNT Growth, and 4) Cool-down. A brief description of the important steps for each phase is as follows. Calcination is the first phase of growth in which oxygen flows into the tube while the temperature ramps up to ~620°C to clean any carbon contamination off the furnace sidewalls or sample and to oxidize the Iron into Iron oxide if it wasn't already. Between ~550°C and 620°C the temperature is increased very slowly in low pressure atmosphere to maintain low thermal mass and uniform temperature to prevent the quartz substrate from cracking as it transitions from α-β phase

at ~573°C. Reduction is the 2nd phase of growth in which hydrogen flows into the tube as the temperature increases from 620°C to the growth temperature between 850-900°C and continues as the tube temperature stabilizes for an additional 10 minutes. This phase reduces the Iron oxide into elemental Iron and the Iron then coalesces into a nanoparticle. Next, the CNT growth phase introduces the flow of carbon containing gas, typically methane or ethanol, for about 30 minutes alongside hydrogen at atmospheric or reduced pressure and is when the CNTs actually begin to grow. Finally, the cool-down phase stops the methane flow and cools down the furnace in Hydrogen or Argon ambient taking care to slowly cool near the phase-change temperature.

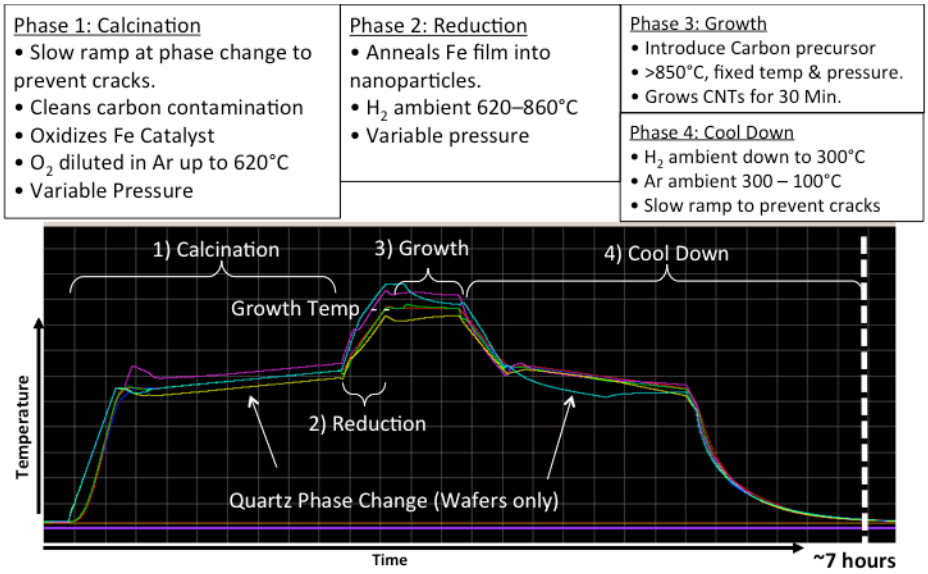

Figure 3: CVD Growth procedure and temperature profile.

Ethanol Growth Recipe Development

Ethanol vs. Methane

Unlike the previous EE412 growth recipes, this effort focuses on using ethanol as a CNT growth precursor. The key difference between the methane carbon precursor used in the previous recipes and ethanol carbon precursor that is the focus of this work is the thermal decomposition pathway for the molecules. As shown in figure 4, the carbon decomposition pathway for methane indirectly results in a molecule containing a C_2 species [Chen 1975] However, the ethanol thermal decomposition pathway for ethanol directly produces a C_2 containing species [Li 2004]. This species is close to the molecule for Acetylene, which is the building block for CNT growth [Eres 2009, Kimura 2013]. In addition ethanol decomposes into water vapor, which weakly etches amorphous carbon in a way that improves the CNT growth yield because amorphous carbon can stop CNT growth prematurely if too much of it accumulates on the catalyst. Therefore, ethanol is a strong choice as a carbon precursor for the growth of CNTs.

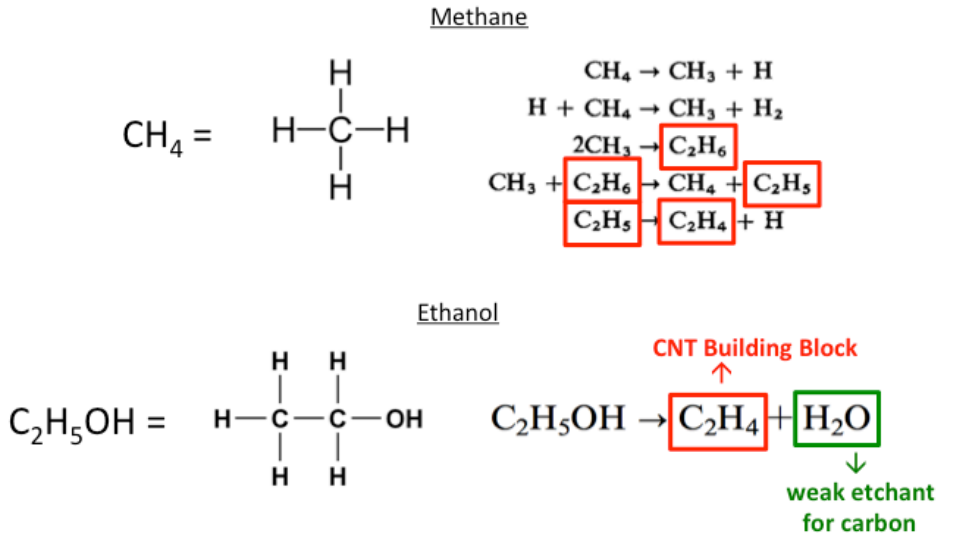

Figure 4: Thermal decomposition of Methane vs. Ethanol. C_2-based molecules are the building block for CNT growth. H_2O is an amorphous carbon etchant

Initial recipe

The initial guess for an ethanol growth condition was a 30 minute atmospheric pressure growth at 865°C, a 50% H_2 and 50% Ar chamber, and a flow of 100sccm Argon through a room temperature ethanol bubbler. The initial results were mixed, as shown in figure 5a. There was excellent nucleation of CNTs from the catalyst stripe, but the CNTs were short and failed to extend the complete distance between stripes. The first instinct to fix this issue was to extend the growth time, so a screening experiment with growth times from 5 minutes to 60 minutes was performed. Four wafers each prepared in the same condition were diced in pieces and pieces from all four wafers were included in each growth. As shown in the results table in figure 5b, for four samples show no trend with tube length vs. time. Therefore a different approach is required.

a)

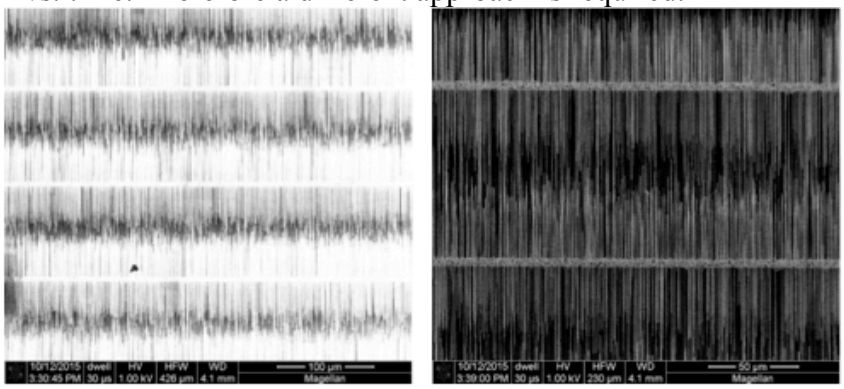

b)

Tube Length (um) vs. Growth Time	5 Min	15 Min	30 Min	60 Min
Sample 1: 3.2Å Fe	26.2	32.92	19	55
Sample 2: 3.2Å Fe	8.4	24.3	6.47	35.7
Sample 3: 3.2Å Fe	20	14.7	7.05	26.3
Sample 4: 3.2Å Fe	13.9	23	11.1	35.7

Figure 5: a) Initial growth condition results with short tubes. b) Growth duration has no effect on CNT length.

Ethanol Vapor Model

Before any effort to improve the growth results by tuning the process condition, it was important to translate between the process knobs available on the tool and the chamber condition. In particular, since the ethanol carbon source is a liquid it is important to model the actual flow of ethanol vapor into the chamber versus the bubbler temperature, pressure, and carrier gas flow. First the vapor pressure of ethanol can be modeled by an Antoine equation as shown in figure 6a, where 'p' is the pressure of vapor in Torr, A, B, and C are Antoine coefficients for ethanol, and T is the temperature of the ethanol liquid. Once the ethanol vapor pressure is know, figure 6b shows the flow of ethanol can be calculated as the argon carrier gas flow into the bubbler multiplied by the fraction of the ethanol partial pressure and the partial pressure of other gases inside the bubbler headspace. Finally, we can model the ethanol flow across the full range of tool parameters and a range of possible conditions is shown in figure 6c and 6d for a 100sccm Ar and 400 sccm Ar flow, respectively. The red circle indicates the initial process condition, so there is a lot of potential to increase the flow of ethanol vapor into the furnace.

a)

$$\log_{10} p = A - \frac{B}{C + T}$$

$A_{Ethanol} = 8.2$
$B_{Ethanol} = 1642.89$
$C_{Ethanol} = 230.3$
T_{Valid}: -20°C → +80°C

b) $$F_{Out} = F_{in} * \frac{P_{EtOH}}{P_{Bubbler} - P_{EtOH}}$$

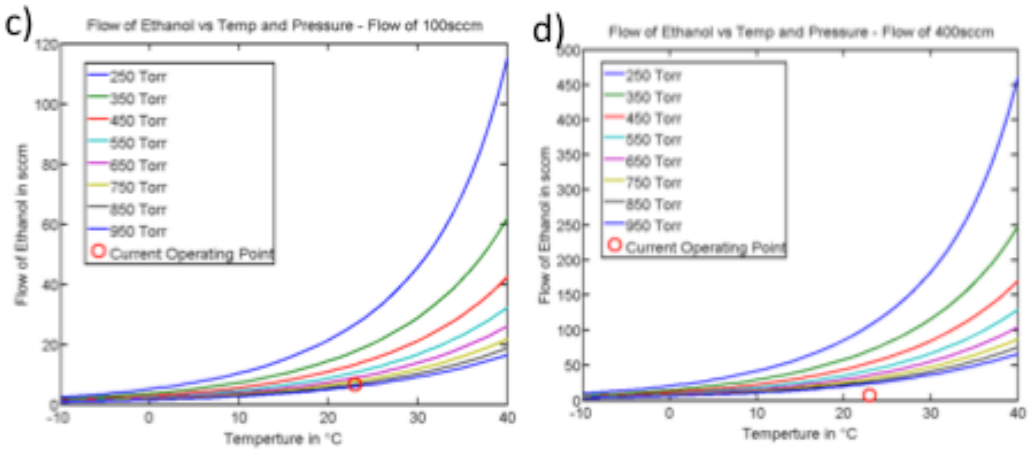

Figure 6: a) Antoine equation and coefficients for ethanol, to calculate partial pressure of ethanol liquid. Coefficients valid from -20°C to +80°C. b) This equation describes the flow of ethanol vapor out of the bubbler. c) and d) show ethanol flow vs. temperature for two different Argon flows through the bubbler. The red circle is the initial growth condition.

Temperature & Ethanol Flow DOE

We expect that two of the largest process parameters will be the growth temperature and the amount of ethanol vapor flowing into the chamber. Therefore we

implemented a 2-parameter DOE investigating growth temperatures between 800°C and 900°C, and ethanol flows between 7.4 sccm and 29.7 sccm (as calculated using the model from figure 6). Our goal was to observe a trend in tube length and/or CNT density, specifically that higher ethanol flows would result in denser CNTs. This goal was largely satisfied. As shown in figure 7's table reporting CNT density vs. growth temperature and ethanol flow, we observe clear trends with both parameters. Lower growth temperature results in very short CNTs despite the presence of some CNT nucleation within the catalyst stripe. Increasing the temperature to 900°C gives significantly better CNT density across a large range of ethanol concentrations. Increasing ethanol flows improves the CNT growth density and tube length across a large range of growth temperatures. Therefore the optimal condition is in the 850-900°C temperature range, and the 22.2 sccm ethanol or higher flow range.

The observed growth density was very interesting. Each growth was performed with four growth pieces taken from four wafers prepared in the same condition, and the density values were extracted over at least 12 microns field of view on each wafer. Also, the location of the density measurement is exactly halfway between the catalyst stripes, which should be the lowest density point. Therefore, these measured densities should give a very fair and accurate representation of the average density across the entire growth piece. The legacy recipe using methane on the FirstNano tool only achieved ~1 CNT/um while the older legacy recipe on the 4" growth furnace in the Philip Wong group lab achieves 5 CNT/um in a good growth. Therefore, right away we are seeing a significant and consistent increase in the density of CNTs that is achievable with this carbon precursor. Actual SEM images of these growth results will be shown later on in figure 10. Much of the future work in this report takes place at 900°C with 22.2 sccm ethanol flow.

Next, having learned of the significance of the growth temperature and ethanol flow, we considered how to push these process knobs further. However, growths above ~925°C have the potential to coat the entire furnace in a soot-like film of amorphous carbon due to the thermal decomposition of the carbon source (a mistake we made earlier this year), which sets a practical upper bound on the growth temperature. On the other hand, it is possible to significantly increase the ethanol flow just by increasing the temperature of the liquid source as described in Figure 6. Several attempts were made to further improve the CNT density by growing with several higher ethanol flows, however as shown in Figure 7 there was no apparent improvement up to the maximum bubbler temperature. In the future we are interested in potentially increasing ethanol flow even more using lower bubbler pressure, however that DOE effort would require extensive work to separate the effect of lower chamber pressure inside the growth chamber and higher ethanol flows.

Sample B11 W2: 3.2Å Fe Liftoff < 1 CNT/um | 1-5 CNT/um | >5 CNT/um

Growth Temp / Ethanol Flow:	7.4 sccm	14.8 sccm	22.2 sccm	29.7 sccm	61.0 sccm
800C			0.6	0	
850C	Short	Short	1.5	6.6	
900C	3.5	8.8	8.8	6.4	6.8
Bubbler Temp	23 C	23 C	23 C	23 C	**40 C**
Ar Flow Through Bubbler	**100 sccm**	**200 sccm**	**300 sccm**	**400 sccm**	300 sccm
Bubbler Pressure	850 Torr	850 Torr	850 Torr	850 Torr	850 Torr

*All density values from SEM averaged over at least 12 um

Figure 7: Growth temperature and ethanol flow DOE shows a growth window at higher temperatures and flows.

Future efforts to improve CNT single-growth density include further increasing the EtOH concentration in the growth chamber, however the best way to do that requires some analysis. Option 1, as shown in figure 8, to decrease the amount of Argon and H2 flowing into the chamber alongside the ethanol would have the effect of taking longer for the chamber to reach equilibrium ethanol concentration. Option 2 is to increase the ethanol flow further (if we could) without changing the ballast gas flow, and would cause the chamber equilibrium concentration to increase while achieving that equilibrium in the same time. To understand which approach if any is worth pursuing, we performed another growth time sweep to understand whether the growth would be finished before the chamber reaches equilibrium. As shown in figure 8b, there was no difference in tube length for a 10 minute growth as compared to a 60 minute growth. Therefore, most of the growth occurs well before the chamber reaches equilibrium. A few more experiments have shown that growth is complete in just a few minutes, making it difficult to tune the condition using Ethanol concentration and indicating the approach to improve growth results requires more careful thought and analysis.

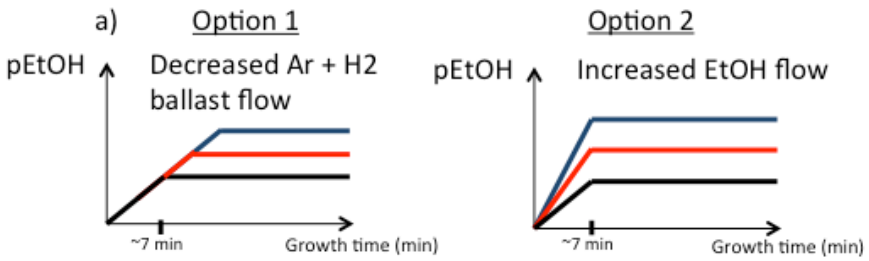

	CNTs per micron			
Growth Time	Sample 1	Sample 2	Sample 3	Sample 4
10 Minutes	10.5	8.3	8.1	8.4
30 Minutes	9.4	6.1	6.3	6.2
60 Minutes	10.7	10.9	8.4	8.3

Figure 9: a) A cartoon illustrating the two options for increasing the ethanol partial pressure. b) a growth time sweep that illustrates that there is no density difference between 10, 30, and 60 minute growths and all of the growth occurs within the first 10 minutes at 900°C with 22.2 sccm ethanol flow.

Another approach to further improve the CNT density is to focus on the catalyst film thickness, which is tightly related to the density and size of the nanoparticles that nucleate the CNTs and therefore may strongly influence the CNT density. However, the evaporated films are extremely thin, only a few angstrom, and it is difficult to say with any certainty what the actual film thickness is since the difference during film evaporation is only roughly 3 seconds. Therefore we cautiously prepared three catalyst thicknesses with 2.5Å, 3.0Å, and 3.5Å of Fe evaporated at 0.33Å/s (by Tom Carver in SNSF) using the liftoff procedure described earlier. Unfortunately, no firm conclusions have been drawn since all three wafers grew reasonably well as shown in figure 9. In order to do this DOE correctly, a wider range of catalyst films must be prepared in order to cover a broader region of the growth window.

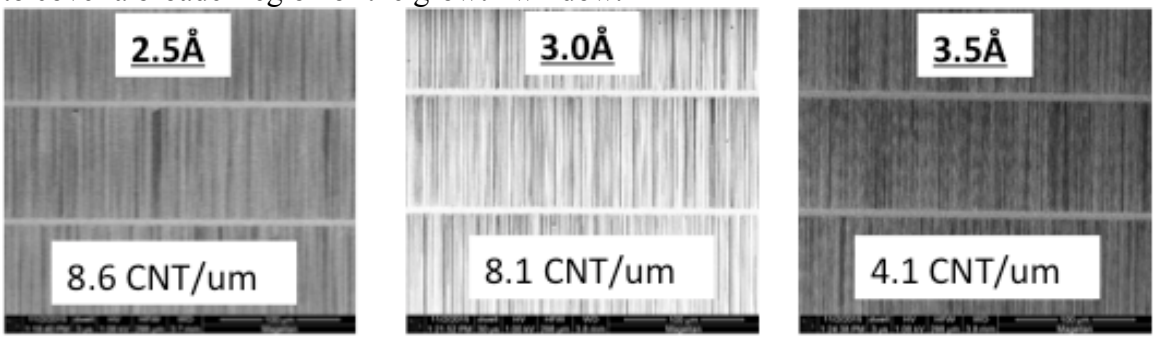

Figure 9: These SEMs illustrate the difficulty in drawing any firm conclusions on the catalyst film's effect of CNT density due to the limited range of films prepared for this project.

Other approaches to improve the CNT single-growth density are going to be under active study for quite some time, and include optimizing the growth pressure, the catalyst material and film thickness, details in the reduction phase of growth, details in calcination phase, and the tiny details in the growth procedure. Ultimately, we would like to understand the mechanisms involved better than they are currently reported in literature which will require a careful and deliberate methodology. This goes beyond the scope of the current work, but will certainly build on these excellent initial results.

Consistency Demonstration

The consistency of our growth result is of primary interest to the SNF labusers who desire a turn-key growth capability. Therefore, we used four wafers prepared in the same condition and divided them into pieces before growing on pieces from all four wafers at the same time repetitively. The first ten growths were done back-to-back using the best-known condition (900°C, 22.2 sccm Ethanol), and as shown in figure 10 the results were excellent. 38 of the 40 samples grew significantly higher than 5 CNTs per micron, and the remaining two grew only slightly less than that. The spread in the densities from 5-10 CNTs per micron can be partially explained by sampling noise in the counting of the CNTs from sample to sample, and there is no clear trend with growth number. Since the 10^{th} run was the 22^{nd} growth on that particular quartz tube and there is no trend indicating degradation in growth density with growth number, this experiment clearly addressed concerns that there is a chamber stability problem. Figure 11 shows SEM images of these growths that illustrate the long, dense CNTs with full surface coverage and gives tangible evidence to the great consistency of these growth results. This same condition was repeated more than one week later after 8 others growths for a

different experiment, an O2 bake of the tube, and a re-fill on the ethanol source – and as shown in figure 10 the results were even better than the average. This result did not change even after dozens of more growths. Therefore the bottom line is that we observe consistent 5-10 CNT/um densities and we observe no obvious stability issues related to the tube cleanliness over multiple weeks and dozens of growths. This is a significant achievement, and accomplishes a primary goal for this EE412 project and FirstNano CNT Furnace startup.

22.2 sccm EtOH, 900°C growth, 760 Torr

	CNTs per micron			
	Sample 1	Sample 2	Sample 3	Sample 4
Run 1:	3.9	8.8	8.0	4.8
Run 2:	7.6	5.4	6.8	5.4
Run 3:	8.0	10.5	8.9	7.6
Run 4:	8.9	9.1	6.0	5.9
Run 5:	7.2	7.2	7.3	6.5
Run 6:	8.8	8.8	7.3	5.2
Run 7:	9.3	5.3	6.6	5.3
Run 8:	9.3	7.9	5.8	6.3
Run 9:	9.3	6.8	5.1	5.4
Run 10:	9.5	8.1	7.2	7.7
1 week later:	10.7	10.9	8.4	8.3

	Sample 1	Sample 2	Sample 3	Sample 4
Mean	8.4	8.1	7.0	6.2

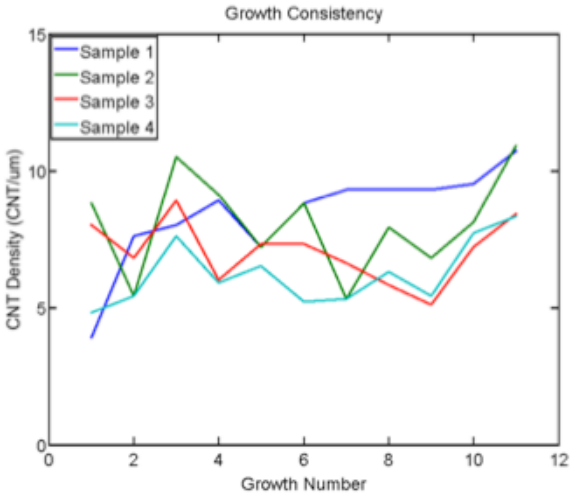

Figure 10: Illustrates the consistent density of aligned CNTs grown with the best condition so far, exceeding our target CNT densities for this project.

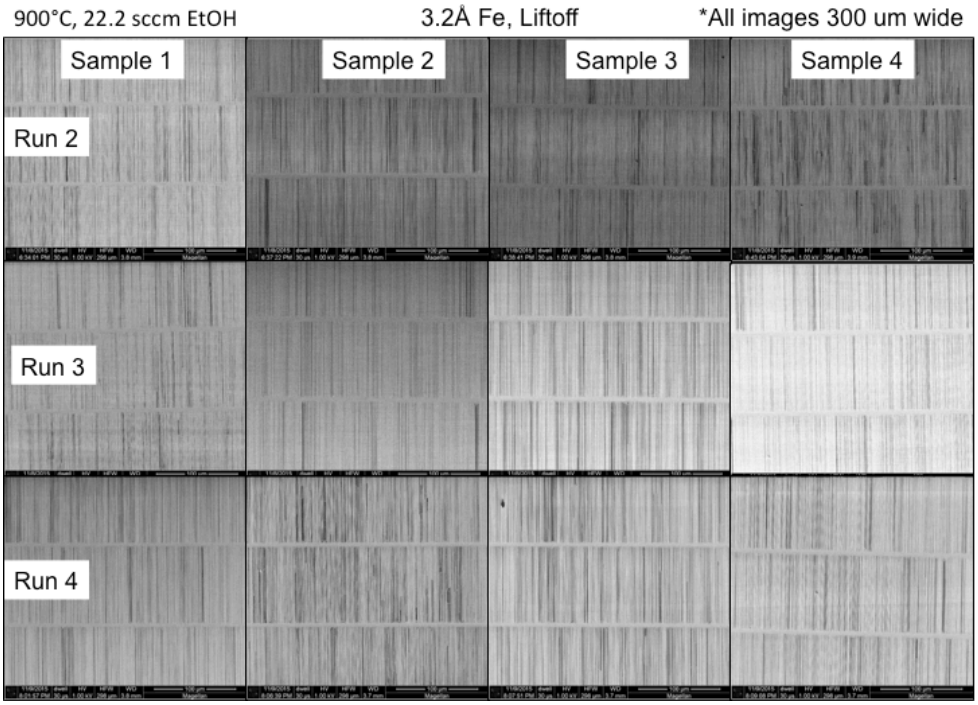

Figure 11: SEM images illustrate the full surface coverage, consistency, and long dense nature of the CNT growth results across 12 samples. These represent the appearance of all 40 samples grown in this consistency demonstration. All images are 300 micron field of view.

Wafer-scale Uniformity Demonstration

The next step was demonstrate the wafer-scalability of the CNT growth density by growing on a 100mm wafer. As described earlier, for a ST-quartz substrate there is a phase change that requires a gradual temperature profile to avoid cracking the wafer. Therefore, as planned the only difference between the pieces recipes we had been working with up until now and the wafer recipe was to respect a slower cool-down rate, while everything up until the end of growth phase remained un-changed. Two wafers were prepared with 3.2Å Fe on them, and both wafers were grown using the best known condition so far. The results were excellent. As shown in Figure 12, the first wafer had an average density of ~6 CNT/um, and uniformity in density across the top, bottom, right, left, and center of the wafer. The second wafer was also above 6 CNTs per micron in the bottom and right regions, however there were unusual signs of having been damaged during processing, and a small fraction of the tubes were misaligned which lowered the CNT density due to CNT collisions. However, even still the problem was not with the growth and the density matched our goals across the entire wafer.

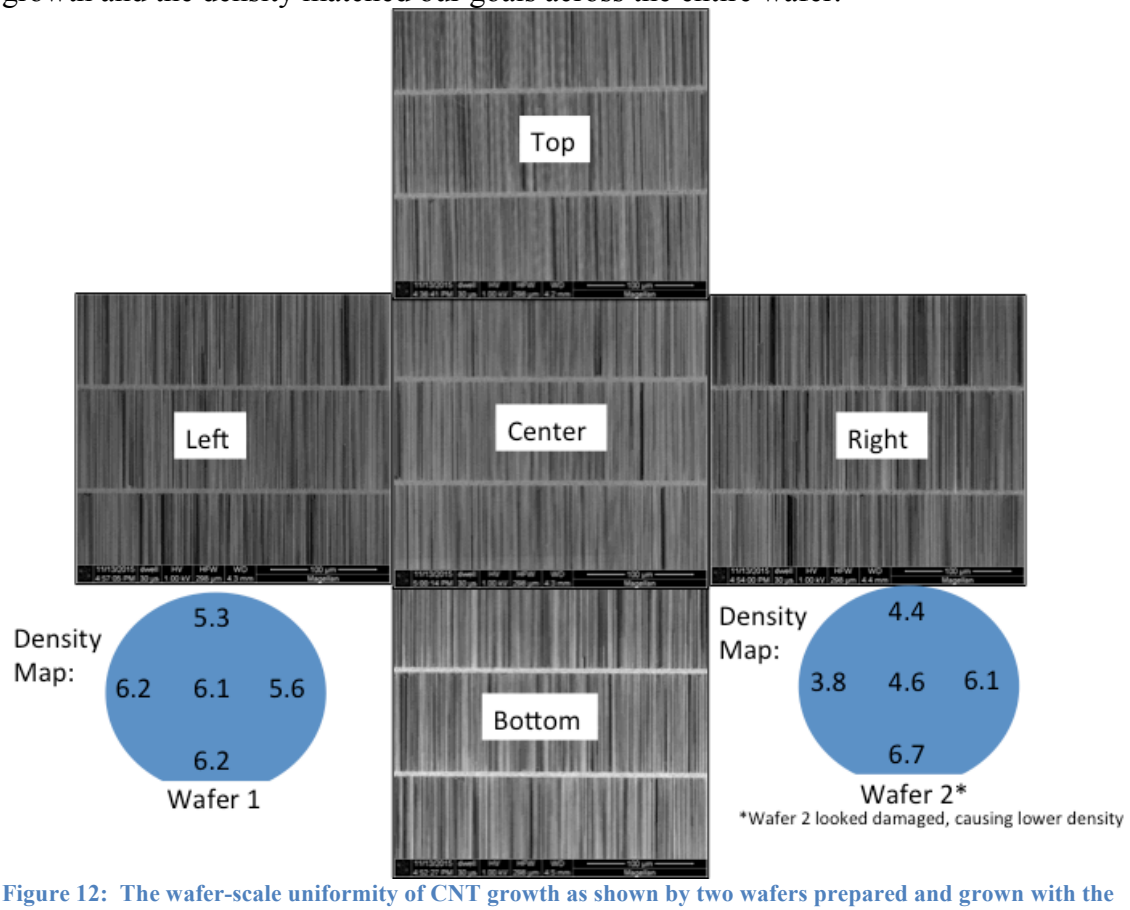

Figure 12: The wafer-scale uniformity of CNT growth as shown by two wafers prepared and grown with the best known conditions. Both wafers exceed our density targets and were very uniform. All SEMs are 300um field of view.

Materials and Electrical Characterization

Finally, it was important to confirm the properties of the as-grown CNTs matched our expectations for their physical properties such as diameter as well as electrical

properties that allow them to be used in CNT-based transistors. As is shown in Figure 13a, the CNT diameter was measured by AFM and a mean diameter value of 1.25nm with a sigma of 0.4nm was observed. This is perfectly consistent with our expectations and similar reports from literature. Next, back-gated field effect transistors were fabricated and measured through a CNT transfer process onto a Si/SiO_2 device processing substrate. The device structure is shown in Figure 13b. Electrical measurement of a narrow device with only semiconducting CNTs is shown in Figure 13c, and confirms that we are growing CNTs that are potentially useful for applications in transistors. Next, several devices were measured that contained some metallic CNTs alongside semiconducting CNTs to confirm we were able to remove the metallic CNTs using a breakdown process, by which we turn off the semiconducting CNTs and pass enough current through the metallic CNTs to oxidize them. As shown in Figure 13d, for both narrow transistors with fewer CNTs and wide transistors with many CNTs we are able to remove the metallic CNTs to achieve significant on/off current ratios. This confirms that the as-grown CNTs have the expected properties and are useful for ongoing research performed inside the SNF.

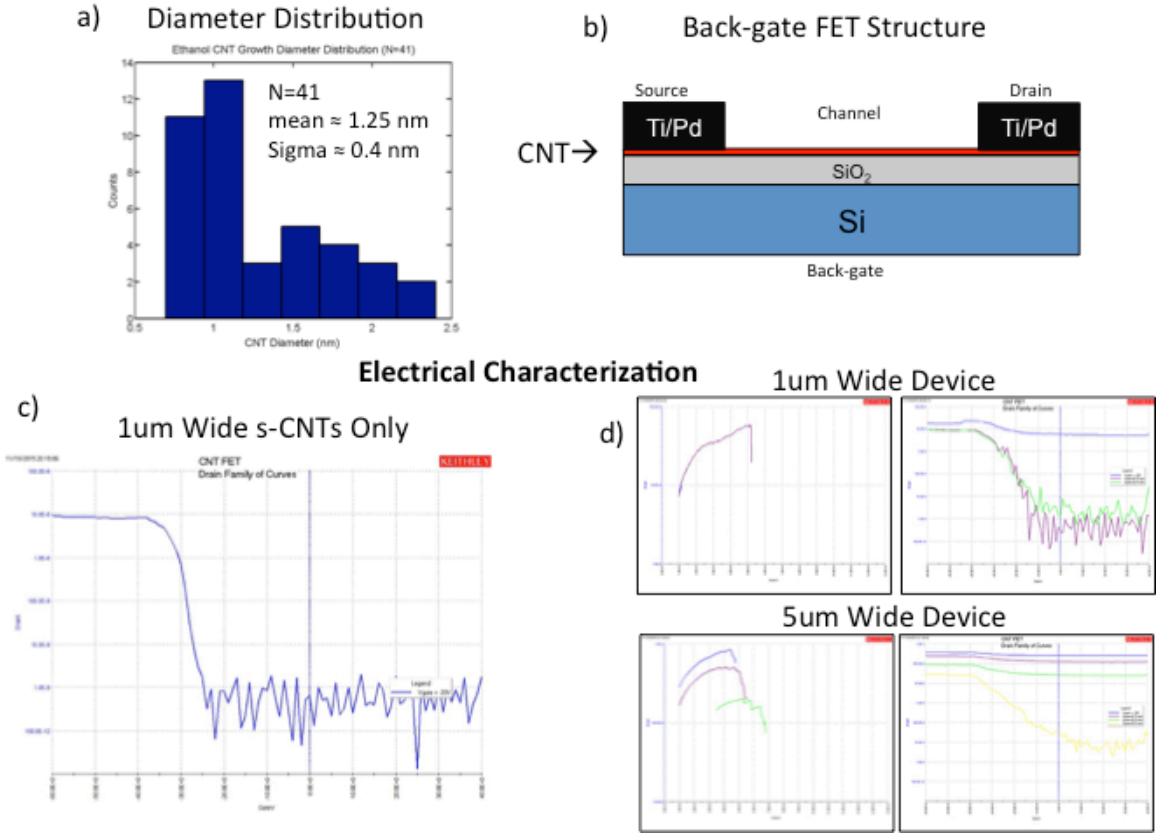

Figure 13: a) Diameter distribution of the as-grown CNTs as measured by AFM. b) Global-back gated device structure for a transistor made using CNTs. Electrical device characterization of c) semiconducting CNTs and d) metallic and semiconducting CNTs that show how metallic CNTs can be selectively removed.

Summary

In summary, we set out to create a turn-key CNT growth recipe for users in the Stanford Nanofabrication Facility using the FirstNano CNT CVD tool. Previously we

have explored the sample preparation procedure and a methane growth recipe that failed to achieve our density goals. In this work we have demonstrated the following 1) an ethanol CNT growth window that achieves 5-10 CNTs per micron, 2) consistency of the growth results and stability of the furnace across several dozen runs, 3) full-wafer coverage and utility of the as-grown CNTs for researchers in the SNF. In addition, we have made a down payment on the kinds of methodical and deliberate process studies that need to be performed to further improve the growth condition by introducing novel elements into growth and understanding the fundamental CVD mechanisms involved. This report summarizes many of the important observations and conclusions from this project, however a more direct document for training users in tool operation and sample preparation has been created as well to facilitate other labmembers in their efforts to grow aligned CNTs.

Acknowledgements

I would like to thank SNF staff members Mary Tang, Robert Chen, Michelle Rincon, and Ted Berg for their support in setting up the FirstNano tool. I would like to thank Ryan Swoboda and Xurong Li for their assistance with the methane growth development earlier in 2015. Finally I would like to thank all of the EE 412 students, mentors, and Wong group members for their constant feedback and helpful conversations.

Citations:

[Chen 1975] C.-J. Chen, M. H. Back, R. A. Back, Canadian Journal of Chemistry, 1975, 53(23): 3580-3590
[Li 2004] J. Li, A. Kazakov, F. Dryer, Journal of Physical Chemistry A, 2004, 108 (38), pp 7671 - 7680
[Eres 2009] G. Eres, et. al., J. Phys. Chem. C, 2009, 113, 15484-15481
[Kimura 2013] H. Kimura, et. al., Scientific Reports, 2013, Vol.3 p.3334